

A revised comprehensive approach for determining the H₂ and D₂ rovibrational population from the Fulcher- α emission in low temperature plasmas

S Briefi*  and U Fantz 

Max-Planck-Institut für Plasmaphysik, Boltzmannstr. 2, 85748 Garching, Germany

E-mail: stefan.briefi@physik.uni-augsburg.de and stefan.briefi@ipp.mpg.de

Received 3 June 2020, revised 16 September 2020

Accepted for publication 13 October 2020

Published 18 December 2020



Abstract

The emission of the Fulcher- α $d^3\Pi_u \rightarrow a^3\Sigma_g^+$ transition is well-known for providing access to the rovibrational population of the hydrogen molecule in low temperature plasmas by means of optical emission spectroscopy. A revised comprehensive approach is developed for the evaluation that omits several simplifying assumptions, which are often made. The rovibrational distribution is directly calculated in the $X^1\Sigma_g^+$ state considering the typically observed hockey-stick population. The projection into the $d^3\Pi_u$ state is performed via vibrationally resolved electron impact excitation cross sections and radiative decay into the $a^3\Sigma_g^+$ is considered via vibrationally resolved transition probabilities. The obtained steady-state population is fitted to the experimentally measured one via varying the population parameters in the electronic ground state. The impact of this evaluation routine compared to the simplified ones is demonstrated both for H₂ and D₂ at two experiments: a standard CW low-power laboratory ICP and the pulsed high-power negative ion source plasma of the Linac4 accelerator at CERN. This assessment demonstrates that especially the simplification of measuring only the first five rotational emission lines (i.e. neglecting the rotational hockey-stick distribution) can affect the evaluation results significantly. In the application example, this leads to an overestimation of the gas temperature up to a factor of nine and to an underestimation of the determined intensity of the full Fulcher- α transition (required for applying collisional radiative models) up to a factor of three.

Keywords: hydrogen, rovibrational population, diatomic molecules, molecular emission

(Some figures may appear in colour only in the online journal)

1. Introduction

The rotational and vibrational excitation of the hydrogen molecule is of high relevance for understanding plasma

chemistry and kinetics in low temperature discharges. A change in the rovibrational distribution can significantly affect several molecular reaction rates. For example, the cross section of negative hydrogen ion formation via dissociative electron attachment increases by several orders of magnitude when the H₂ or D₂ molecule is excited to higher vibrational states [1]. The rotational excitation has a similar effect as the rate only depends on the total internal energy of the molecule and not on the particular rotational or vibrational excitation state [2].

* Author to whom any correspondence should be addressed.



Original content from this work may be used under the terms of the [Creative Commons Attribution 4.0 licence](https://creativecommons.org/licenses/by/4.0/). Any further distribution of this work must maintain attribution to the author(s) and the title of the work, journal citation and DOI.

The vibrational excitation of the hydrogen molecules plays also an important role in plasma kinetics of the divertor region in fusion plasmas. Due to the low electron temperature especially near the divertor target plates, hydrogen molecules can have a long penetration depth and lead to molecular assisted recombination [3], a process that requires vibrational excitation [4]. Enhancing the plasma recombination in this region is beneficial as it reduces the heat load and ion bombardment of the target plates.

For measuring the rovibrational excitation directly in the electronic ground state of the hydrogen molecule, rather sophisticated diagnostic methods are required. For example, anti-Stokes Raman scattering (CARS) spectroscopy [5–7], resonantly enhanced multi-photon ionization [8], VUV laser absorption spectroscopy (where the VUV laser radiation is generated by four-wave sum-frequency mixing of two pulsed dye laser beams in a mercury vapor oven) [9, 10] or laser induced fluorescence (where the laser radiation is generated via stimulated CARS) [11, 12] were applied. Due to the complexity and high costs of these diagnostics, such investigations are scarce.

A much more widespread diagnostic technique for obtaining the ground state rovibrational population in an indirect way is optical emission spectroscopy (OES) of the H₂ or D₂ Fulcher- α transition ($d^3\Pi_u \rightarrow a^3\Sigma_g^+$) due to the simple measurement setup [13, 14]. The single emission lines can be resolved with a high-resolution spectrometer what makes the determination of the rovibrational distribution in the excited $d^3\Pi_u$ state straightforward (typically the first five rotational levels within the first four vibrational states are measured). However, in order to derive information about the rovibrational population of the electronic ground state from the excited state, the relevant population and depopulation processes have to be considered.

Historically, not much data was available about these processes and several simplifying assumptions were made for determining the rovibrational ground state population. Despite the availability of most of the required data nowadays, these routines are still often applied due to their simplicity. However, the validity and consequences of the assumptions have barely been assessed in literature. This paper establishes a fundamental and comprehensive approach for evaluating the Fulcher- α transition where simplifying assumptions are not required. Furthermore, the impact of each assumption made with the simpler approaches is assessed in detail.

The focus is also put on the determination of the intensity of the whole Fulcher- α emission (defined as wavelength-integrated spectral radiance [$\text{m}^{-3}\text{s}^{-1}$]) which can be derived from the excited state population. This quantity is required for the evaluation of the plasma emission via collisional radiative (CR) models of the H₂ or D₂ molecule as such models are typically not rovibrationally resolved and only the whole electronic state is considered (see for example [15] and references therein). In addition, the full intensity is required for determining the flux of molecular hydrogen emerging from plasma-facing components in fusion devices [16], yielding insights into plasma edge fuelling and general plasma properties [17, 18].

In the first section of the paper, general properties of the Fulcher- α transition are discussed briefly. The different approaches typically taken towards determining the ground state rotational and vibrational distributions are also described including the necessary assumptions. Afterwards, the comprehensive approach is outlined both for H₂ and D₂: concerning the rotational distribution, it relies on calculating the full rovibrational distribution directly in the ground state and transferring it to the $d^3\Pi_u$ state via vibrationally resolved electron impact excitation cross sections. The resulting population is fitted to the experimentally determined one, which is measured up to high rotational quantum numbers ($N' = 12$ in hydrogen and $N' = 13$ in deuterium). For determining the vibrational distribution, a vibrationally resolved population model is set up. This allows in general the consideration of several population and depopulation channels. In the last section of the paper, the comprehensive and the simplified approaches are compared for OES measurements both of H₂ and D₂ discharges carried out at two different experimental setups: a typical low pressure low temperature CW ICP and the pulsed high-power negative ion source plasma of the Linac4 accelerator at CERN.

2. The Fulcher- α transition of molecular hydrogen

2.1. General considerations

The Fulcher- α spectrum is distributed over a wide wavelength range between 520 and 770 nm but the most prominent part lies at 590–650 nm. The emission is typically the most intense one of the hydrogen molecule being the reason why it is ideally suited for diagnostic purposes. A description of the detailed properties of the Fulcher- α transition and the corresponding electronic states have already been described several times in the literature (see for example [13, 19]). Hence, only a short summary is given here.

Because of λ -doubling, the upper electronic state is split into the $d^3\Pi_u^+$ and $d^3\Pi_u^-$ states. The Q branch of the Fulcher- α transition originates from the $d^3\Pi_u^-$ state only whereas the P and R branch originate from the $d^3\Pi_u^+$ state due to optical selection rules. The P and R branch are typically not considered for diagnostic purposes, as the $d^3\Pi_u^+$ state is strongly perturbed by other electronic states [20, 21] leading to anomalies in the intensities of emitted lines [22].

The dissociation limit of H₂ to H(1s) and H(2s) is located at 4.75 eV and therefore between the energy levels of the vibrational states $v' = 3$ and $v' = 4$ in the $d^3\Pi_u^-$ state [23, 24]. For energy levels above this limit, predissociation occurs. This leads to non-radiative decay of the states and therefore the Fulcher- α emission gets considerably weaker for transitions involving states with $v' \geq 4$ [25]. For deuterium the dissociation limit is between the states $v' = 4$ and $v' = 5$ and consequently, transitions from $v' \geq 5$ are much weaker [20]. Hence, the investigations presented in this paper are limited to the first four vibrational quantum numbers of the $d^3\Pi_u^-$ state. In order to obtain a good signal to noise ratio, the measurement of the rovibrational population is furthermore restricted to the diagonal vibrational transitions ($v' = v''$) as they represent the most

intense emission bands within the whole electronic transition. The wavelength of the Q branch emission lines (often abbreviated with the letter Q followed by the rotational quantum number) can be found in tabulated form in [26] for hydrogen and in [27] for deuterium up to high rotational quantum numbers.

In low temperature discharges, the excitation of the $d^3\Pi_u^-$ state predominantly occurs via electron impact excitation out of the ground state $X^1\Sigma_g^+$ [13, 19]. During this process, the rotational quantum number N (it should be used instead of J as the electronic states belong to Hund's coupling case b) is not altered as the selection rule $\Delta N = 0$ holds. The contribution of quadrupole excitation that would allow for a change in N is less than 10% [13]. This means, that the rotational distribution is preserved during electron impact excitation.

As the lifetime of the considered vibrational levels is only around 40 ns both for H₂ and D₂ [28], the rovibrational population in the excited $d^3\Pi_u^-$ state is not changed via repopulation processes (like inelastic heavy particle collisions or other processes) in low pressure discharges. It has been estimated that the population of the $d^3\Pi_u^-$ state via radiative decay of higher electronic levels is around 10% in a discharge with high electron temperatures and densities of $T_e = 100\text{--}200$ eV and $n_e \approx 10^{18} \text{ m}^{-3}$ [13]. In low temperature plasmas, the effect of cascades can be considered smaller and therefore typically negligible. Nevertheless, it should be kept in mind that population from radiative cascades might play a role.

2.2. Evaluating the Fulcher- α emission

2.2.1. Simplified approach: rotational population and T_{gas} . The energy difference of the rotational levels in the electronic ground state of hydrogen is below 0.1 eV. Therefore, they are dominantly populated via heavy particle collisions in low pressure low temperature plasmas and a Boltzmann distribution according to the gas temperature T_{gas} can be assumed. Due to the special properties of the population and depopulation processes described in the last section (excitation without changing N , no redistribution in excited state), the rotational population determined from the Fulcher- α Q branch emission is a direct image of the rotational distribution in the electronic ground state of the hydrogen molecule. This has been exploited by using it as gas temperature diagnostic (see for example [19, 29–33]).

The intensity $\epsilon^{v',N'}$ of a rovibrational emission line originating from the level with quantum numbers v' and N' in the $d^3\Pi_u^-$ state is determined from OES. Typically, only the first five rotational lines (sometimes even less) within a vibrational state are considered as they provide the best signal-to-noise ratio. The line intensity is proportional to

$$\epsilon^{v',N'} \propto g S^{N'} \exp\left(\frac{E(N') - E(N' = 1)}{k_B T_{\text{rot}}}\right), \quad (1)$$

where g denotes the degeneracy arising from the nuclear spin and according to $(2N' + 1)$. $S^{N'}$ is the Hönl–London factor, $E(N')$ the energy of the level with quantum number N' , and T_{rot} the rotational temperature of the Boltzmann population in the

excited $d^3\Pi_u^-$ state [34]. Plotting $\ln\left[\epsilon^{v',N'}/(gS^{N'})\right]$ in against the energy of the states yields the rotational temperature via the slope of a linear fit. In the typical approach, the determined rotational temperature $T_{\text{rot}}(d^3\Pi_u^-, v')$ is projected into the $X^1\Sigma_g^+, v = 0$ state according to the ratio of the rotational constants B_v of the vibrational states (which can be found in [35]):

$$T_{\text{gas}} = T_{\text{rot}}(X^1\Sigma_g^+, v = 0) = \frac{B_v(X^1\Sigma_g^+, v = 0)}{B_v(d^3\Pi_u^-, v')} T_{\text{rot}}(d^3\Pi_u^-, v'). \quad (2)$$

It has been observed, that the back-projection of the four individual rotational temperatures $T_{\text{rot}}(d^3\Pi_u^-, v' = 0, \dots, 3)$ does not give the same results for $T_{\text{rot}}(X^1\Sigma_g^+, v = 0)$ [33]. Typically, the obtained value decreases with vibrational quantum number and the best agreement to independently determined gas temperature values is obtained from $T_{\text{rot}}(d^3\Pi_u^-, v' = 2)$ for H₂ and from $T_{\text{rot}}(d^3\Pi_u^-, v' = 1)$ for D₂ [33].

During the back-projection of the rotational population according to equation (2) the simplification is made, that the population of all $d^3\Pi_u^-, v'$ states solely arises from the $X^1\Sigma_g^+, v = 0$ state. Contributions from levels with $v > 0$ are neglected. An assessment of this simplification yielded that it may be justified for the vibrational quantum numbers $v' = 2$ and 3 but it may fail for $v' = 0$ and 1 (both for H₂ and D₂) [36].

2.2.2. Simplified approach: vibrational population. In order to derive the vibrational population in the excited state, a summation over the population of the individual rotational levels within one vibrational state is carried out. This is typically done based on extrapolating the rotational population according to $T_{\text{rot}}(d^3\Pi_u^-, v')$ (which is typically determined from the first five rotational levels as described in the last paragraph) to states with $N' > 5$.

For connecting the vibrational population in the $d^3\Pi_u^-$ state with the one of the ground state, the electron impact excitation process $X^1\Sigma_g^+ \rightarrow d^3\Pi_u^-$ as well as the transition probabilities for spontaneous emission to the $a^3\Sigma_g^+$ state must be considered. Historically, neither vibrationally resolved electron impact excitation cross section nor vibrationally resolved transition probabilities were available in literature. Therefore, the excitation was assumed to arise solely out of the $X^1\Sigma_g^+, v = 0$ state, and differences in the radiative lifetimes of the excited vibrational states were neglected as well [37]. A more sophisticated approach is applying the Franck–Condon (FC) approximation both for the excitation and radiative decay into the $a^3\Sigma_g^+$ state [31, 38]. Here, a vibrational population is calculated in the electronic ground state according to a Boltzmann distribution and the two population and depopulation processes of the $d^3\Pi_u^-$ state are considered with the corresponding FC factors. The calculated vibrational distribution in the excited state is fitted via varying the vibrational temperature in the ground state.

The FC approach implies two simplifications: first, it assumes a constant electron dipole transition moment for the $d^3\Pi_u^- \rightarrow a^3\Sigma_g^+$ radiative decay (however, the dipole transition moment is not constant, see [39]). Second, the reduced energy threshold for the excitation process out of higher vibrational levels of the $X^1\Sigma_g^+$ state is not taken into account. In order to consider the last point, scaling factors for the FC factors were introduced [38].

In order to avoid both simplifications, vibrationally resolved electron impact excitation cross sections as well as vibrationally resolved transition probabilities were calculated for H₂ and applied to the Fulcher- α transition [40]. However, only a very limited amount of rotational states was considered (Q1–Q5 for $v' = 0$, Q1–Q3 for $v' = 1, 2, 3$). Nevertheless, it has been demonstrated that especially at low electron temperatures where the mean electron energy is close to the excitation threshold, the FC approximation shows significant deviations from the vibrationally resolved cross sections [40].

2.2.3. Comprehensive approach. In order to overcome the above-mentioned assumptions that have to be made for determining the rovibrational population, a fundamental and comprehensive approach is established for H₂ and D₂. It is based on calculating both the relative rotational and vibrational distribution directly in the electronic ground state of the hydrogen molecule considering the hockey-stick distribution. The projection into the $d^3\Pi_u^-$ level is performed via vibrationally resolved electron impact excitation cross sections and radiative decay into the $a^3\Sigma_g^+$ state is considered via vibrationally resolved transition probabilities. In the following, the comprehensive approach is described in detail.

In low pressure plasmas, a Boltzmann distribution is usually present for the vibrational H₂ states up to $v = 8$ in the electronic ground state [7, 10, 41] whereas for higher levels, a slight overpopulation (maximum for $v = 10$ by about a factor of two compared to the Boltzmann distribution) was measured [11]. However, a small overpopulation in such high-lying levels does not contribute significantly to the electron impact excitation rates into the $d^3\Pi_u^-$, $v' \leq 3$ levels and can be disregarded.

One process among others that can cause both rotational and vibrational excitation is surface recombination of hydrogen atoms (see [12] and references therein). A part of the binding energy of the formed molecule is converted into internal excitation leading to Boltzmann distributions with a temperature in the range of several thousand Kelvin. In order to consider this effect, a two-temperature vibrational distribution is used (as often applied in literature):

$$n(v, X^1\Sigma_g^+) = (1 - \beta_{\text{vib}}) \frac{n(v, T_{\text{vib},1})}{\sum_v n(v, T_{\text{vib},1})} + \beta_{\text{vib}} \frac{n(v, T_{\text{vib},2})}{\sum_v n(v, T_{\text{vib},2})}$$

with

$$n(v, T) = \exp \left[-\frac{E(v) - E(v=0)}{k_B T} \right]. \quad (3)$$

$T_{\text{vib},1}$ describes the temperature of the cold vibrational population (arising from plasma processes in general), $T_{\text{vib},2}$ the temperature of the hotter one (arising from the surface recombination) and β_{vib} the weighting factor between them. $E(v)$ is the energy of the vibrational level with quantum number v . The vibrational population is normalized according to $\sum_v n(v, X^1\Sigma_g^+) = 1$.

The dominant process determining the rotational population in the electronic ground state are inelastic heavy particle collisions resulting in a Boltzmann distribution according to the gas temperature of the plasma. Surface recombination or other processes can lead to a second Boltzmann distribution [12] and the rotational levels within the vibrational state v can be described via a two-temperature population:

$$n^v(N, X^1\Sigma_g^+) = (1 - \beta_{\text{rot}}) \frac{n^v(N, T_{\text{rot},1})}{\sum_N n^v(N, T_{\text{rot},1})} + \beta_{\text{rot}} \frac{n^v(N, T_{\text{rot},2})}{\sum_N n^v(N, T_{\text{rot},2})}$$

with

$$n^v(N, T) = g \exp \left[-\frac{E(N) - E(N=1)}{k_B T} \right]. \quad (4)$$

In contrast to the vibrational population, the statistical weight g of the particular level arising from the degeneracy ($2N + 1$) and from the nuclear spin (alternating 1 and 3 for hydrogen; 2 and 1 for deuterium) must be considered. According to equation (4), the population is normalized to $\sum_N n^v(N, X^1\Sigma_g^+) = n(v, X^1\Sigma_g^+)$. It has been demonstrated by an independent determination of the gas temperature that the population according to $T_{\text{rot},1}$ reflects the gas temperature [36].

As both the hot rotational and vibrational population arise from surface recombination, $T_{\text{rot},2}$ is set equal to $T_{\text{vib},2}$ and $\beta_{\text{rot}} = \beta_{\text{vib}} = \beta$. The rovibrational population is calculated for all 14 (21 for D₂) bound vibrational states and for the first 15 (20 for D₂) rotational states within a vibrational level (or up to the last bound rotational state for high vibrational levels). The energy levels are taken from [42] both for H₂ and D₂. The rovibrational population is calculated according to equations (3) and (4) in a way that the measurements by [12, 43] are reproduced qualitatively.

The projection of the rovibrational population out of the $X^1\Sigma_g^+$ state into the $d^3\Pi_u^-$ level is performed via a full set of vibrationally resolved electron impact excitation rate coefficients, which are deduced from the corresponding cross section assuming a Maxwellian electron energy distribution function (assuming that the rotational population is unchanged during excitation [13]). As vibrationally resolved cross sections are not available in the literature, they have been calculated according to the semi-classical Gryzinski method [44] both for H₂ and D₂ [45]. With this approach, the relative rotational population within the first four vibrational levels in the $d^3\Pi_u^-$ state is determined as this population is

also experimentally accessible. It should be noted, that the electron temperature is required as additional input from the experiment.

In general, it would be possible to use the above approach also for determining the relative vibrational population by considering the radiative lifetime of the particular vibrational levels in the $d^3\Pi_u^-$ state what has been done by [40]. However, in some special cases, radiative decay from higher lying states [13] or stepwise excitation out of the metastable $c^3\Pi_u(v=0)$ level (see [46] for a more detailed discussion on this point) may become relevant for the population of the $d^3\Pi_u^-$ state. Although this is not the case for the plasmas investigated in this paper, one might want to include such effects in the future. Therefore, a vibrationally resolved population model has been set up both for H_2 and D_2 [45] using the flexible solver Yacora [15]. In the current version, it balances electron impact excitation from the $X^1\Sigma_g^+$ into the $d^3\Pi_u^-$ state and depopulation via radiative decay into the $a^3\Sigma_g^+$ (the vibrationally resolved transition probabilities are taken from [24]) for all bound vibrational levels within the three electronic states. As input, the model requires the vibrational population in the electronic ground state which is calculated as described in equation (3) and the electron temperature.

For fitting the measurements with the calculations, an iterative process must be applied: first, a simultaneous least-square fit of the measured rotational population in the first four vibrational levels of the $d^3\Pi_u^-$ state is performed via varying the parameters $T_{rot,1}$, $T_{rot,2}$ and β in the $X^1\Sigma_g^+$ state. In the next step, a summation over the rotational population in each vibrational level of the $d^3\Pi_u^-$ state is carried out. The obtained vibrational distribution is normalized to the $d^3\Pi_u^-, v'=0$ level and a fitting with the population model is performed via varying $T_{vib,1}$ (as input parameters the values of $T_{vib,2} = T_{rot,2}$ and β determined in the previous step and the electron temperature are taken). The obtained value of $T_{vib,1}$ is used as new input for the first fitting step and iteratively, the fitting steps are repeated until convergence is obtained (typically after two or three iterations).

The full intensity of the Fulcher- α Q branch is calculated as follows: from the relative rovibrational population of the $d^3\Pi_u^-(v'=0, 1, 2, 3)$ states and the absolute intensity of the intense Q1 emission line (Q2 for D_2) in each vibrational state, the absolute intensity of the four diagonal vibrational transitions ($v' = v''$) is determined. From the population model, a factor comparing the intensity of these four diagonal transitions to the full Fulcher- α intensity can be derived. It depends on the rovibrational population as well as the electron temperature and lies between 1.08 (for low values of $T_{vib,1}$ and T_e) and 6.5 (for high values of $T_{vib,1}$ and low T_e). The factor allows scaling the actually measured intensity of the diagonal transitions to the intensity of the full transition. If the CR model does not distinguish between the $d^3\Pi_u^-$ and the $d^3\Pi_u^+$ state, one can also use the determined rovibrational parameters for the $d^3\Pi_u^+$ state in order to calculate the intensity in the P and R branches. However, one should be aware that this approach neglects the line intensity anomalies due to perturbations present in this state leading to erroneous intensities for these branches.

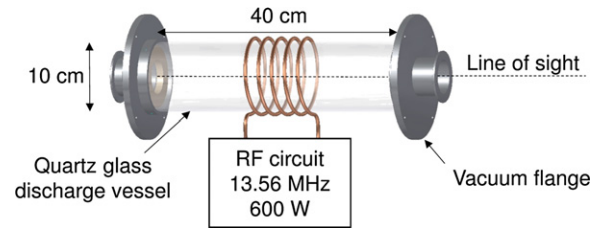


Figure 1. Sketch of the experimental setup of the low-power ICP.

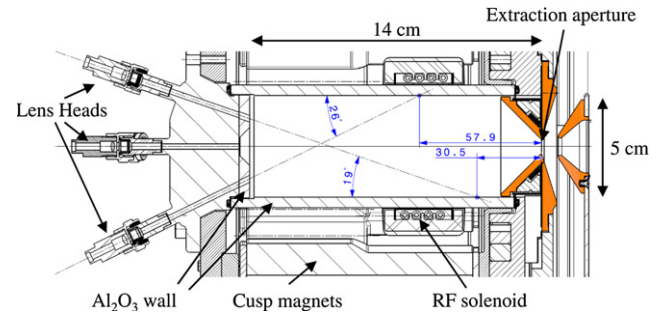


Figure 2. Sketch of the experimental setup of CERN's Linac4 ion source.

3. Experimental setup and diagnostics

The comprehensive approach for evaluating the Fulcher- α transition is demonstrated at two different experiments: first, at a low-power inductively coupled CW plasma consisting of a cylindrical quartz vessel with a length of 40 cm and a diameter of 10 cm. Figure 1 shows a sketch of the setup. The experiment is operated with an RF frequency of 13.56 MHz and a power of 600 W. For the investigations presented in this paper a pressure of 1 Pa was used. OES measurements are performed at a line of sight (LOS), which is directed along the central axis of the discharge vessel. An intensity calibrated high-resolution spectrometer is applied, having a Gaussian apparatus profile with a full width at half maximum (FWHM) of 18 pm at a wavelength of 650 nm.

The second experiment is the Linac4 H^- ion source at CERN. Its plasma is generated also with inductive RF coupling ($f = 2$ MHz) but with a much higher RF power of 50 kW. The cylindrical discharge vessel is made out of alumina and has a length of 14 cm and a diameter of 5 cm (see figure 2, more details on the setup can be found in [47]). OES measurements can be conducted at three different view ports. For the investigations presented in this paper, only the axial LOS was used. The discharge at the Linac4 ion source is operated at 3 Pa pressure in pulsed mode with a repetition rate of 2 Hz. The discharge duration was set to 900 μs . An intensity calibrated high-resolution spectrometer equipped with an intensified CCD camera is used for OES. The apparatus profile of this setup has a Lorentzian shape with a FWHM of 8 pm at a wavelength of 650 nm. Concerning the evaluation of the Fulcher- α spectrum, the Lorentzian line profile is rather disadvantageous as it causes overlapping of nearby lines due to the broad wings despite the small FWHM. Therefore, several lines must be excluded from the evaluation.

As explained in section 2.2.3, the electron temperature is required as additional input parameter for the calculation of the rovibrational populations. It can be obtained from OES measurements of the Balmer series of atomic hydrogen followed by an evaluation with the CR model Yacora. More details on the model and the evaluation procedure can be found in [47, 48] respectively.

4. Application of the comprehensive approach

In order to demonstrate the benefit of applying the comprehensive approach described in section 2.2.3, exemplary measurements were carried out both in H_2 and D_2 . The obtained results are described first. It should be noted, that a multitude of different physical processes leads to the observed rovibrational distributions. These processes are not discussed in detail, as this is way beyond of the scope of this paper. Exemplary, such discussions can be found in [12, 49] or [41]. A systematic comparison to the evaluation routines used in the literature up to and the comprehensive approach now is made at the end of this section in order to assess the impact of the simplifications.

4.1. Low-power ICP – hydrogen

The OES measurements of the Fulcher- α transition in H_2 were carried out recording the first 12 rotational lines within the first four vibrational levels of the $d^3\Pi_u^-$ state. Only the Q10 and Q11 lines of $v' = 1$ and Q10 of $v' = 2$ could not be evaluated as they overlap with other emission lines, and the Q9 to Q12 lines of $v' = 3$ were below the detection limit. Figure 3 shows the resulting measured rovibrational population together with the result of the fitting procedure described in section 2.2.3. For the fit, the rotational levels with $N' > 10$ in the $v' = 2$ state and with $N' > 3$ in the $v' = 3$ state are not considered as they are influenced by predissociation leading to a reduced population density (this effect is not considered in the simulation). The obtained fitting parameters are $T_{\text{rot},1} = 600 \pm 25$ K, $T_{\text{rot},2} = 6700 \pm 700$ K and $\beta = 0.174 \pm 0.005$ (the values are rounded to 5 K, 100 K, and 0.001 resp.) It can be seen that the fit works very well for all considered states. The accuracy of the fitting is high for all three parameters as the two-temperature distribution is clearly evident and enough data points are present both in the low and high-temperature part.

Figure 4 shows the vibrational population in the $d^3\Pi_u^-$ state obtained from summation over the extrapolated measured rotational distribution as well as the one obtained from the population model for varying values of $T_{\text{vib},1}$. Concerning the simulation for the experimentally obtained electron temperature of 4.5 eV, a large variation of the relative vibrational distribution is obtained for low values of $T_{\text{vib},1}$ whereas at high values, the distribution converges. Therefore, a high fitting accuracy with low error is only possible for $T_{\text{vib},1} \lesssim 4000$ K. Between 4000 K and 6000 K, the accuracy is limited to ± 500 K, for $T_{\text{vib},1} \gtrsim 6000$ K, only a lower bound can be given. A good fit between measurement and calculation

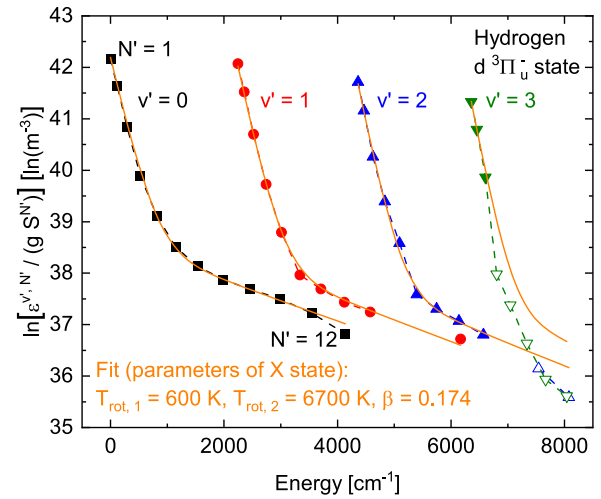


Figure 3. Measured (symbols) and fitted (line) rotational population of the first four vibrational levels in the H_2 $d^3\Pi_u^-$ state obtained in the low-power ICP for 1 Pa pressure and 600 W RF power. The states with $N' > 10$ in the $v' = 2$ state and with $N' > 3$ in the $v' = 3$ state (open symbols) are not considered for the fit as their population is reduced due to predissociation.

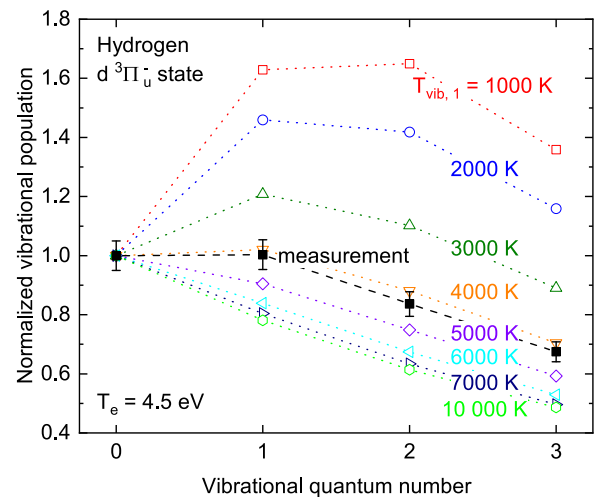


Figure 4. Measured (full symbols) and simulated (open symbols) vibrational population of the first four levels in the H_2 $d^3\Pi_u^-$ state obtained in the low-power ICP. The vibrational population has been calculated considering the experimentally determined electron temperature of 4.5 eV (the electron density is $3.4 \times 10^{16} \text{ m}^{-3}$).

is obtained for $T_{\text{vib},1} = 4000 \pm 500$ K (result rounded to full 500 K).

For the obtained parameters, the scaling factor from the measured intensity of the first four diagonal vibrational transitions to the full Fulcher- α transition has a value of 1.99. This yields an intensity of $1.25 \times 10^{20} \text{ m}^{-3}\text{s}^{-1}$ when both the $d^3\Pi_u^-$ and $d^3\Pi_u^+$ states are taken into account and $6.87 \times 10^{19} \text{ m}^{-3}\text{s}^{-1}$, when only the non-perturbed $d^3\Pi_u^-$ state is considered.

The rovibrational population of the $X^1\Sigma_g^+$ state determined by the fitting procedure is shown in figure 5 for the first six vibrational levels. As already pointed out, this distribution agrees qualitatively with the ones measured in [12, 43].

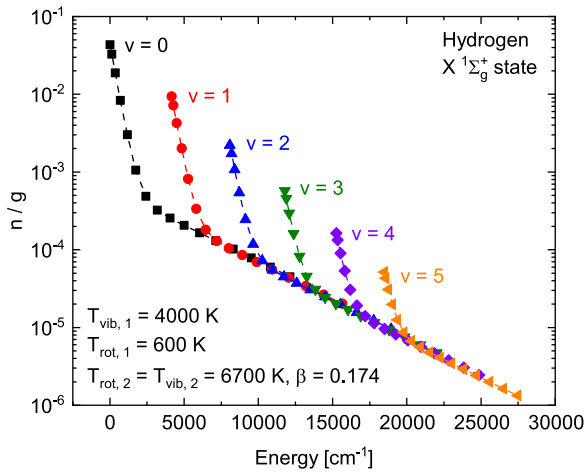


Figure 5. Rovibrational population of the $\text{H}_2\text{X}^1\Sigma_g^+$ state determined from the fitting the experimental data in the low-power ICP. Only the first six vibrational levels are shown.

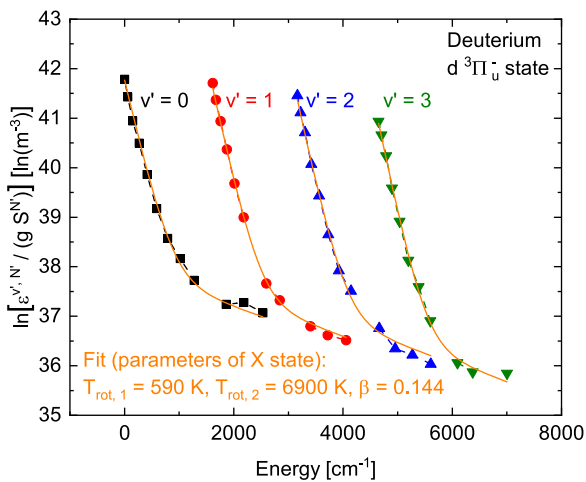


Figure 6. Measured (symbols) and fitted (line) rotational population of the first four vibrational states in the $\text{D}_2 d^3\Pi_u^-$ state obtained in the low-power ICP for 1 Pa pressure and 600 W RF power.

4.2. Low-power ICP—deuterium

In D_2 , the first 13 rotational lines within the first four vibrational levels of the $d^3\Pi_u^-$ state were recorded. Excluded from the fitting due to an overlap with other lines were the Q10 line of $v' = 0$, Q7 and Q9 of $v' = 1$, Q9 of $v' = 2$ and Q9 and Q12 of $v' = 3$. Figure 6 shows the measured and simulated rovibrational population of the $d^3\Pi_u^-$ state. The fitting results are $T_{\text{rot},1} = 590 \pm 25$ K, $T_{\text{rot},2} = 6900 \pm 900$ K and $\beta = 0.144 \pm 0.005$ and similar to H_2 a very good agreement between fit and measurement is observed. However, as for deuterium the energy difference in the rotational states is lower due to the higher mass, more levels are populated according to $T_{\text{rot},1}$ and less levels follow $T_{\text{rot},2}$. Therefore, the fitting accuracy is high for $T_{\text{rot},1}$ and β , but the fitting error of $T_{\text{rot},2}$ is larger compared to H_2 .

The vibrational distribution calculated from the measurement and obtained from the population model is shown in

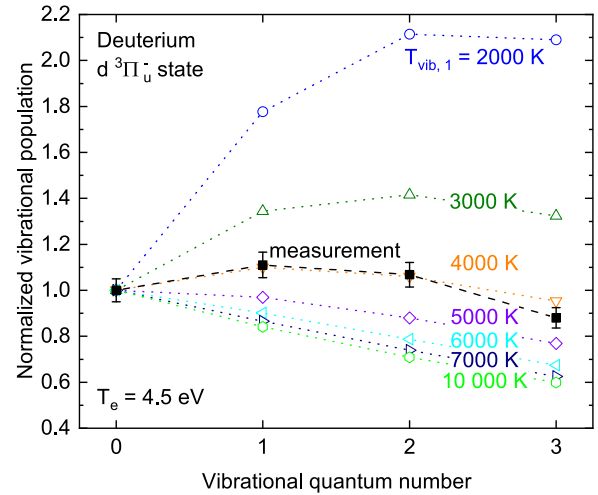


Figure 7. Measured (full symbols) and simulated (open symbols) vibrational population of the first four vibrational states in the $\text{D}_2 d^3\Pi_u^-$ state obtained in the low-power ICP. The vibrational population has been calculated considering the experimentally determined electron temperature of 4.5 eV (the electron density is $4.3 \times 10^{16} \text{ m}^{-3}$).

figure 7 for the experimentally determined electron temperature of 4.5 eV. The fit yields $T_{\text{vib},1} = 4000 \pm 500$ K. Similar to H_2 , the relative distribution changes significantly for low values of $T_{\text{vib},1}$ and converges for higher ones. This means that also in D_2 , only a lower bound of the vibrational temperature can be given for $T_{\text{vib},1} \gtrsim 6000$ K.

The factor for scaling the measured diagonal transitions to the full Fulcher- α emission is 2.97, yielding a total intensity of $1.62 \times 10^{20} \text{ m}^{-3}\text{s}^{-1}$ when both the $d^3\Pi_u^-$ and $d^3\Pi_u^+$ states are considered ($8.18 \times 10^{19} \text{ m}^{-3}\text{s}^{-1}$, when only the non-perturbed $d^3\Pi_u^-$ state is considered).

4.3. High-power ICP—deuterium

For the high-power discharge of the Linac4 ion source, the same rotational lines are acquired as for the low-power ICP. However, as described in section 3, the problem of line overlap is larger due to the Lorentzian apparatus profile of the spectroscopic setup. This leads to more scatter in the determined rotational population what can be seen in figure 8, where the measured rovibrational population of the $d^3\Pi_u^-$ state of D_2 is plotted together with the resulting fit (several lines have to be excluded due to overlap). In addition, the signal-to-noise ratio is worse as for the low-power ICP, for example, the rotational lines above Q4 of the $v' = 3$ state are all below the detection limit. Nevertheless, also for the high-power discharge, the two-temperature distribution is evident. For the fit, some special characteristics of the plasma have to be considered: due to the short discharge duration of only 900 μs heating up of the heavy particles is prevented [50]. This is reflected in the cold rotational temperature of $T_{\text{rot},1} = 275 \pm 40$ K obtained from the fitting. This agrees within the error bars with the ambient temperature of 300 K, which reflects the temperature of the inlet gas. The fitting furthermore yields $T_{\text{rot},2} = 5800 \pm 400$ K and $\beta = 0.908 \pm 0.005$. Compared to the low-power ICP, the

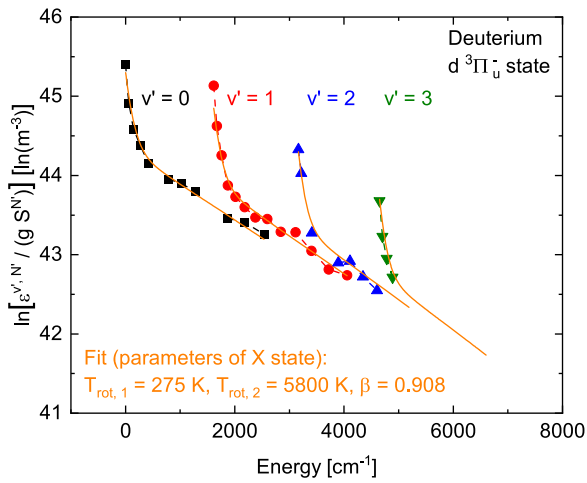


Figure 8. Measured (symbols) and fitted (line) rotational population of the first four vibrational states in the D_2 $d^3\Pi_u^-$ state obtained in the high-power ICP for 3 Pa pressure and 50 kW RF power.

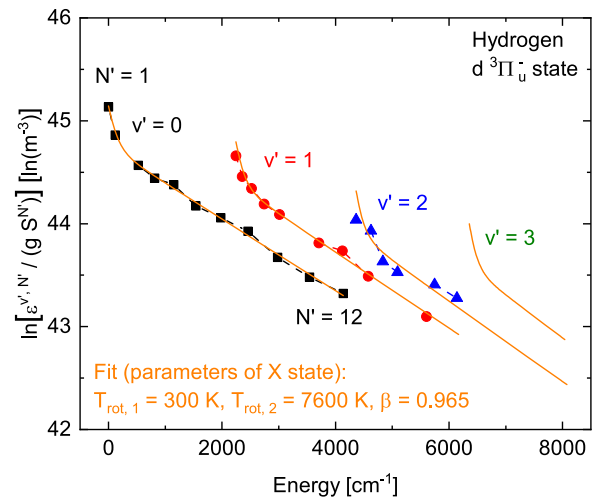


Figure 10. Measured (symbols) and fitted (line) rotational population of the first four vibrational states in the H_2 $d^3\Pi_u^-$ state obtained in the high-power ICP for 3 Pa pressure and 50 kW RF power.

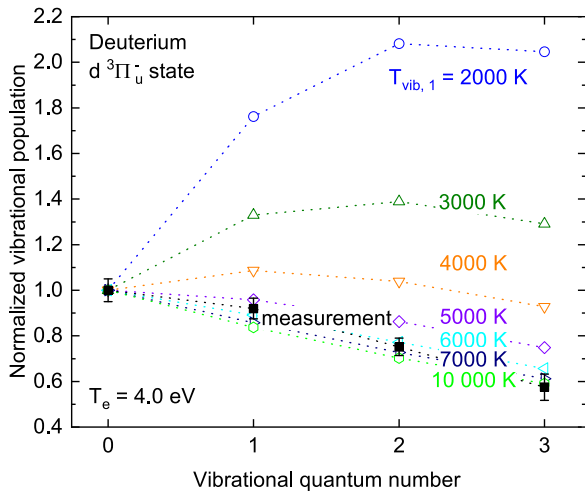


Figure 9. Measured (full symbols) and simulated (open symbols) vibrational population of the first four vibrational states in the D_2 $d^3\Pi_u^-$ state obtained in the high-power ICP. The vibrational population has been calculated considering the experimentally determined electron temperature of 4.5 eV (the electron density is $3 \times 10^{19} \text{ m}^{-3}$).

share of the hot population is more than a factor of six higher leading to a high fitting accuracy also for $T_{\text{rot},2}$ in D_2 .

Figure 9 shows the vibrational distribution determined from the measurement and the population model for the experimentally obtained electron temperature of 4.0 eV. The measured values can be fitted with $T_{\text{vib},1} = 6000 \text{ K}$. However, as this is close to the insensitive range it must be considered as lower bound. It should be noted, that this value is similar to the one of $T_{\text{rot},2} = T_{\text{vib},2}$. For the vibrational population, a two-temperature distribution is therefore barely present. The calculation of the full Fulcher- α intensity yields $1.39 \times 10^{22} \text{ m}^{-3}\text{s}^{-1}$ ($7.03 \times 10^{21} \text{ m}^{-3}\text{s}^{-1}$, when only the $d^3\Pi_u^-$ state is considered).

The strong differences in the rovibrational distributions determined in the high-power and the low-power ICP point

towards different processes being relevant for the rovibrational population in the electronic ground state what is reasonable due to the short discharge duration vs CW operation. However, a detailed discussion of these processes is beyond the scope of this paper.

4.4. High-power ICP – hydrogen

For the H_2 isotope, the rotational lines of the $v' = 3$ levels could not be recorded as they were below the detection limit. In contrast to D_2 , the hockey-stick distribution is only weakly present in the rotational population (see figure 10). This arises from the fact that the energy difference of the particular rotational levels is larger compared to deuterium. As only the $N' = 1$ state in each vibrational level follows the cold rotational temperature this point might be erroneously considered as outlier. Therefore, the rovibrational distributions of D_2 have been discussed first where the rotational population according to the ambient temperature is clearly present. Nevertheless, a fit of the distribution measured in H_2 can still be carried out when $T_{\text{rot},1}$ is manually set to the ambient temperature of 300 K. The resulting values are $T_{\text{rot},2} = 7600 \pm 400 \text{ K}$ and $\beta = 0.965 \pm 0.005$. For the vibrational distribution, only a lower bound of $T_{\text{vib},1} = 6000 \text{ K}$ can be given similarly to D_2 (see figure 11). Fulcher- α intensity is $1.14 \times 10^{22} \text{ m}^{-3}\text{s}^{-1}$ ($5.88 \times 10^{21} \text{ m}^{-3}\text{s}^{-1}$, when only the $d^3\Pi_u^-$ state is considered).

4.5. Assessment of the simplified approaches

In the following, the evaluation with the comprehensive approach described in the last sections is compared to those typically performed in the literature up to now. In general, there are five major differences or simplifications:

- Fitting the rotational temperature only at the first five Q lines compared to the full hockey-stick fitting up to Q12 (Q13 for D_2). The back-projection after equation (2) is

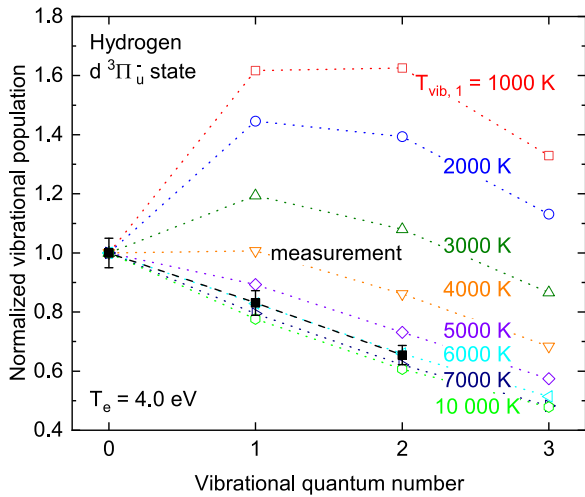


Figure 11. Measured (full symbols) and simulated (open symbols) vibrational population of the first four vibrational states in the H_2 $d^3\Pi_u^-$ state obtained in the high-power ICP. The vibrational population has been calculated considering the experimentally determined electron temperature of 4.5 eV (the electron density is $3 \times 10^{19} \text{ m}^{-3}$).

performed in both cases for determining the gas temperature. For the simplified approach, T_{gas} is evaluated from the $d^3\Pi_u^-$, $v' = 2$ state in H_2 ($v' = 1$ in D_2) according to [33].

- Performing the back-projection of the rotational temperature to the ground state according to equation (2) in order to determine T_{gas} versus calculating the rotational population directly in the ground state (in both cases the hockey-stick fitting is performed).
- Determining the relative vibrational distribution in the $d^3\Pi_u^-$ state by extrapolating the rotational population fitted to the first five Q lines compared to the full hockey-stick fitting.
- Modelling the vibrational population in the $d^3\Pi_u^-$ state via applying the scaled FC principle as described in [38] versus the full vibrationally resolved population model. The rotational hockey-stick distribution is considered in both cases.
- The evaluation of the full Fulcher- α intensity when the hockey-stick rotational population is not considered and the FC approximation is applied compared to the intensity obtained from the comprehensive approach.

Concerning point (a), the comparison between the comprehensive and simplified approach is summarized in table 1. In general, the rotational temperature and therefore T_{gas} is overestimated when the hockey-stick distribution is neglected [36]. The amount of overestimation strongly depends on the weighting factor β . For low values of β , all first five rotational levels follow the cold rotational distribution and the fitting yields the same temperature for both the comprehensive and simplified approach. This is the case for the low-power ICP in D_2 . In H_2 , the value of β is only 20% higher but this is enough that the levels $N' = 4$ and 5 are already influenced by the hot part of the distribution. Therefore, the gas temperature determined with

Table 1. T_{gas} obtained from the comprehensive approach (abbreviated CA) and the simplified approach (abbreviated SA). The values of the weighting factor of the hot part of the hockey-stick distribution are also given. For the high-power ICP in H_2 , the gas temperature was manually set to 300 K as explained in section 4.4.

Discharge	Gas	T_{gas} (K)		β
		With CA	With SA	
Low-power ICP	H_2	600	750 (+25%)	0.174
	D_2	590	590 ($\pm 0\%$)	0.144
High-power ICP	H_2	300 (set)	2650 (+883%)	0.965
	D_2	275	890 (+324%)	0.908

the simplified approach is overestimated by 25%. For very high values of β , the rotational temperature derived from the simplified approach is much higher (by 883% for the high-power ICP in H_2) than the one obtained with the comprehensive approach. In this case, most of the rotational levels actually follow the hot distribution and thus the rotational temperature does not reflect T_{gas} any more.

For point (b), no difference in the gas temperature values is present when applying the simplified or the comprehensive approach within the error bars for all exemplary investigations. This means, that the excited states are dominantly populated from the $X^1\Sigma_g^+$, $v = 0$ state even for higher vibrational temperatures as in the case of the high-power ICP.

The deviation of the relative vibrational populations in the $d^3\Pi_u^-$ state derived with the comprehensive and simplified approaches (point (c)) is summarized in table 2. Only the levels $v' = 1$ to 3 are contained as the distribution is normalized to the population of the $v' = 0$ level in each case. In general, neglecting the hot part of the hockey-stick distribution leads to an underestimation of the relative vibrational population. However, for low values of β as obtained in the low-power ICP, the contribution from this part to the over-all population is low and virtually the same vibrational distribution is determined. The small deviation of a few per cent arises from the fitting of the rotational distribution, which is done in the ground state for the comprehensive approach and in the excited state for the simplified approach. An exception is the $d^3\Pi_u^-$, $v' = 3$ state in H_2 where the simplified approach underestimates the population density by 18% because fitting the rotational temperature to the first five Q lines includes the levels $N' = 4$ and 5 which have a reduced population density due to predissociation. For high values of β as in the case of the high-power ICP, disregarding the hot part of the rotational distribution means neglecting a considerable share of the over-all population. This is partly compensated by the overestimated rotational temperature (this effect is stronger in H_2 than in D_2 , see table 1). In total, the underestimation reaches more than 20% in the case of H_2 and more than 30% for D_2 .

For point (d), the vibrational population derived from the measurement can both be fitted with the FC approximation and the newly set up population model for H_2 (the population model represents the relative trend slightly better). However, as summarized in table X, the vibrational temperature obtained from the FC approach yields values that are 25%

Table 2. Deviation of the relative vibrational population obtained from the simplified approach where hockey-stick distribution is neglected (abbreviated SA) to the one from the comprehensive approach (abbreviated CA). The values of the weighting factor of the hot part of the hockey-stick distribution are also given.

Discharge	Gas	Deviation of SA from CA			β
		$v' = 1$	$v' = 2$	$v' = 3$	
Low-power ICP	H ₂	+1%	+5%	−18%	0.174
	D ₂	+1%	+3%	+4%	0.144
High-power ICP	H ₂	−20%	−25%	n.a.	0.965
	D ₂	−3%	−32%	−33%	0.908

Table 3. Vibrational temperature obtained from the comprehensive (abbreviated CA) and the simplified approach (abbreviated SA).

Discharge	Gas	$T_{vib,1}$ (K)	
		With CA	With SA
Low-power ICP	H ₂	4000	5000 (+25%)
	D ₂	4000	4500 (+13%)
High-power ICP	H ₂	≥ 6000	7500 (+25%)
	D ₂	≥ 6000	Fit not possible

higher than the ones obtained from the population model (a similar trend has been reported by [40]). For D₂, fitting of the vibrational population using the FC approach is difficult as the trend of the measured normalized population is not well reflected in the calculation. In the case of the low-power ICP, the population of the $v' = 1$ level fits well to $T_{vib} = 4000$ K whereas at higher v' values, the calculation with $T_{vib} = 5000$ K is matched. Increasing the tolerance level for accepting a fit, a value of 4500 ± 1000 K can still be given. This is not the case for the high-power ICP: for $v' = 1$ the fit would yield $T_{vib} = 6000$ K whereas for $v' = 3$ it would be 9000 K (the convergence of the vibrational population with high temperatures is not so strong with the FC approach). This makes a fit of the vibrational temperature impossible. It should furthermore be noted, that for the high-power ICP, fitting the experimentally determined relative vibrational distribution with the simulated one requires the consideration of the hockey-stick rotational distribution. If the hot part is neglected, a fit is not possible as the relative populations of $v' = 2$ and 3 derived from the measurements are below the converged vibrational population obtained for high values of $T_{vib,1}$.

A comparison of the simplified and comprehensive approach concerning the intensity ϵ of the full Fulcher- α transition (point (e)) is compiled in table 3. In the case of the low-power ICP and H₂, the simplified approach yields an intensity which is slightly higher than the one of the comprehensive approach. In general, the factor for scaling the intensity from the measured vibrational diagonal transitions to the full transition is only very weakly dependent on the vibrational temperature. This means that the small deviations of $T_{vib,1}$ as summarized in table 4 have basically no impact on the determined value of ϵ .

Table 4. Intensity of the full Fulcher- α transition derived with the comprehensive (abbreviated CA) and the simplified approach (abbreviated SA). Both the $d^3\Pi_u^+$ and $d^3\Pi_u^-$ states are considered.

Discharge	Gas	ϵ (m ^{−3} s ^{−1})	
		With CA	With SA
Low-power ICP	H ₂	1.25×10^{20}	1.33×10^{20} (+6%)
	D ₂	1.62×10^{20}	1.26×10^{20} (−22%)
High-power ICP	H ₂	1.14×10^{22}	6.64×10^{21} (−42%)
	D ₂	1.39×10^{22}	3.96×10^{21} (−72%)

Starting from the full intensity derived from the comprehensive approach and neglecting the hot part of the hockey-stick distribution reduces ϵ by 18%. However, setting the cold rotational temperature to the higher value of the gas temperature determined with the simplified approach raises ϵ again more or less by the same factor. Therefore, the two opposed effects present in the simplified approach cancel each other in this case. Coincidentally, the same intensity is obtained as with the comprehensive approach for the low-power ICP in H₂. For the low-power ICP in D₂, the gas temperature is not underestimated with the simplified approach as explained above. Therefore, the observed underestimation of ϵ by 22% can directly be attributed to the missing hot part of the rotational population.

Disregarding the hot part for the high-power ICP leads to an underestimation of ϵ by 52% in H₂. This is only partly compensated by the higher gas temperature and in total, the simplified approach underestimates the intensity of the full Fulcher- α transition by 42%. The same general trends are observed for D₂, but the compensation due to the higher gas temperature is much smaller than in H₂.

5. Summary

A comprehensive approach for evaluating the rovibrational population of the H₂ and D₂ electronic ground state via OES measurements of the Fulcher- α transition has been outlined. It relies on the calculation of the rovibrational distributions directly in the $X^1\Sigma_g^+$ state by considering the typically observed hockey-stick populations. The projection into the upper $d^3\Pi_u^-$ level of the Fulcher- α transition is performed via vibrationally resolved electron impact excitation cross sections that have been calculated according to the semi-classical Gryzinski method. Radiative decay into the $a^3\Sigma_g^+$ state is considered via vibrationally resolved transition probabilities.

This comprehensive approach omits several assumptions and simplifications that are typically made up to now during the evaluation of the Fulcher- α emission. In order to quantify the impact of these assumptions, the simplified and comprehensive approaches were applied to two different discharges (both for H₂ and D₂), a typical CW low-power laboratory ICP and the pulsed high-power ICP of CERN'S Linac4 ion source. In general, the comprehensive approach can be applied for all cases and the measured rovibrational populations can be fitted very well.

The first simplification typically made is evaluating only the first five rotational states (sometimes even less) within a vibrational level of the $d^3\Pi_u^-$ state. In the comprehensive approach, the first 12 rotational states for H_2 (13 for D_2) are included in the evaluation allowing for a consideration of the rotational hockey-stick distribution. The investigations showed that the simplification leads to an erroneous determination of the rotational temperature and therefore of T_{gas} in general. Depending on the relevance of the hot part of the rotational population, the gas temperature can be strongly overestimated by almost a factor of nine in the case of the pulsed high-power ICP in H_2 . Neglecting the two-temperature distribution also leads to an underestimation of the population in the single vibrational states (in maximum by more than 30%), which is derived from summation over the rotational levels. This makes it impossible to fit this population by modelling in some cases. In turn, the calculated intensity of the full Fulcher- α transition, which is required for further evaluation by CR models, is underestimated up to a factor of three.

The assumption that the $d^3\Pi_u^-$ state is dominantly populated out of the $X^1\Sigma_g^+$, $v = 0$ level holds for the investigated cases. However, the validity of this assumption depends on the vibrational distribution of the ground state and on the electron temperature and electron density in general. Therefore, this assumption should be carefully checked for each application case.

The simplification of using the FC principle both for the electron impact excitation and the radiative decay leads to an overestimation of the determined vibrational temperatures in general (for H_2 by 25%). Furthermore, the trend of the measured relative vibrational population is not reflected in the simulation for D_2 what made the evaluation impossible in the case of the high-power discharge.

In summary, it can be stated that the comprehensive approach provides a much better insight into the rovibrational population of the hydrogen molecule compared to the simplified approaches taken up to now. Especially considering only the first five rotational levels can lead to a significant error on the determined rovibrational population and the calculated full intensity of the Fulcher- α transition. Although it increases the experimental effort—but still by far not to the level of the direct measurement methods as described in section 1, it is highly advisable to take the rotational emission lines up to high quantum numbers into account.

Acknowledgements

The authors would like to thank D Wunderlich for deriving the vibrationally resolved electron impact excitation cross section according to the Gryzinski method and for setting up the Yacora model for the vibrational population. They would also like to thank J Lettry for giving the opportunity to perform measurements at the Linac4 ion source and the Deutsche Forschungsgemeinschaft (DFG) for their support within the project BR 4904/1-1.

ORCID iDs

S Briefi  <https://orcid.org/0000-0003-2997-3503>

U Fantz  <https://orcid.org/0000-0003-2239-3477>

References

- [1] Celiberto R, Janev R K, Laricchiuta A, Capitelli M, Wadehra J M and Atems D E 2001 *At. Data Nucl. Data Tables* **77** 161–213
- [2] Wadehra J M 1984 *Phys. Rev. A* **29** 106–10
- [3] Fantz U, Reiter D, Heger B and Coster D 2001 *J. Nucl. Mater.* **290–293** 367–73
- [4] Kukushkin A S, Krashenninnikov S I, Pshenov A A and Reiter D 2017 *Nucl. Mater. Energy* **12** 984–8
- [5] Meulenbroeks R F G, Engeln R A H, van der Mullen J A M and Schram D C 1996 *Phys. Rev. E* **53** 5207–17
- [6] Péalat M, Taran J P E, Bacal M and Hillion F 1985 *J. Chem. Phys.* **82** 4943–53
- [7] Wagner D, Dikmen B and Döbele H F 1998 *Plasma Sources Sci. Technol.* **7** 462–70
- [8] Bonnie J H M, Eenshuistra P J and Hopman H J 1988 *Phys. Rev. A* **37** 1121–32
- [9] Stutzin G C, Young A T, Schlachter A S, Leung K N and Kunkel W B 1989 *Chem. Phys. Lett.* **155** 475–80
- [10] Stutzin G C, Young A T, Döbele H F, Schlachter A S, Leung K N and Kunkel W B 1990 *Rev. Sci. Instrum.* **61** 619–21
- [11] Mosbach T, Katsch H-M and Döbele H F 2000 *Phys. Rev. Lett.* **85** 3420–3
- [12] Vankan P, Schram D C and Engeln R 2004 *Chem. Phys. Lett.* **400** 196–200
- [13] Farley D R, Stotler D P, Lundberg D P and Cohen S A 2011 *J. Quant. Spectrosc. Radiat. Transfer* **112** 800–19
- [14] Astashkevich S A, Käning M, Käning E, Kokina N V, Lavrov B P, Ohl A and Röpcke J 1996 *J. Quant. Spectrosc. Radiat. Transfer* **56** 725–51
- [15] Wunderlich D, Giacomini M, Ritz R and Fantz U 2020 *J. Quant. Spectrosc. Radiat. Transfer* **240** 106695
- [16] Brezinsek S, Greenland P T, Mertens P, Pospieszczyk A, Reiter D, Samm U, Schweer B and Sergienko G 2003 *J. Nucl. Mater.* **313–316** 967–71
- [17] Hollmann E M, Brezinsek S, Brooks N H, Groth M, McLean A G, Pigarov A Y and Rudakov D L 2006 *Plasma Phys. Control. Fusion* **48** 1165–80
- [18] Bykov I *et al* 2020 *Phys. Scr. T* **171** 014058
- [19] Lavrov B P 1980 *Opt. Spectrosc.* **48** 375–80
- [20] Dieke G H 1935 *Phys. Rev.* **48** 610–4
- [21] Dieke G H and Blue R W 1935 *Phys. Rev.* **47** 261–72
- [22] Kovacs I, Lavrov B P, Tyutchev M V and Ustimov V I 1983 *Opt. Spectrosc.* **54** 537–8
- [23] Sharp T E 1971 *At. Data Nucl. Data Tables* **2** 119–69
- [24] Fantz U and Wunderlich D 2006 *At. Data Nucl. Data Tables* **92** 853 full data set available as IAEA INDC(NDS)-457 report–973
- [25] Yamasaki D, Kado S, Xiao B, Iida Y, Kajita S and Tanaka S 2006 *J. Phys. Soc. Japan* **75** 044501
- [26] Dieke G H 1972 *The Hydrogen Molecule Wavelength Tables of Gerhard Heinrich Dieke* ed H M Crosswhite (New York: Interscience (Wiley-Interscience))
- [27] Freund R S, Schiavone J A and Crosswhite H M 1985 *J. Phys. Chem. Ref. Data* **14** 235–383
- [28] Astashkevich S A and Lavrov B P 2002 *Opt. Spectrosc.* **92** 818–50
- [29] Lavrov B P, Ostrovskii V N and Ustimov V I 1979 *Opt. Spectrosc.* **47** 30–4
- [30] Lavrov B P and Tyutchev M V 1984 *Acta Phys. Hung.* **55** 411–26

- [31] Sobolev N N (ed) 1989 *Electron-excited Molecules in Nonequilibrium Plasma Proceedings of the Lebedev Physics Institute, Academy of Sciences of the USSR* vol 179 (Commack, NY: Nova Science Publishers)
- [32] Tomasini L, Rousseau A, Gousset G and Leprince P 1996 *J. Phys. D: Appl. Phys.* **29** 1006–13
- [33] Fantz U 2004 *Contrib. Plasma Phys.* **44** 508–15
- [34] Herzberg G 1950 *Molecular Spectra and Molecular Structure, I. Spectra of Diatomic Molecules* vol 2 (New York: D van Nostrand Company)
- [35] Huber K P and Herzberg G 20899 *NIST Chemistry Web-Book, NIST Standard Reference Database Number 69* ed P J Linstrom and W G Mallard (Gaithersburg MD: National Institute of Standards and Technology) <http://webbook.nist.gov> (retrieved May 20, 2016)
- [36] Briefi S, Rauner D and Fantz U 2017 *J. Quant. Spectrosc. Radiat. Transfer* **187** 135–44
- [37] Lavrov B P and Proskhin V P 1985 *Opt. Spectrosc.* **58** 317–20
- [38] Fantz U and Heger B 1998 *Plasma Phys. Control. Fusion* **40** 2023–32
- [39] Staszewska G and Wolniewicz L 1999 *J. Mol. Spectrosc.* **198** 416–20
- [40] Xiao B, Kado S, Kajita S and Yamasaki D 2004 *Plasma Phys. Control. Fusion* **46** 653–68
- [41] Vankan P, Schram D C and Engeln R 2004 *J. Chem. Phys.* **121** 9876–84
- [42] Pachucki K and Komasa J 2015 *J. Chem. Phys.* **143** 034111
- [43] Gabriel O, Schram D C and Engeln R 2008 *Phys. Rev. E* **78** 016407
- [44] Gryzinski M 1965 *Phys. Rev.* **138** A336–58
- [45] Wunderlich D 2020 private communication
- [46] Fantz U, Heger B, Wunderlich D, Pugno R and Asdexupgradeteam A U 2003 *J. Nucl. Mater.* **313–316** 743–7
- [47] Briefi S, Mattei S, Rauner D, Lettry J, Tran M Q and Fantz U 2017 *New J. Phys.* **19** 105006
- [48] Wunderlich D, Dietrich S and Fantz U 2009 *J. Quant. Spectrosc. Radiat. Transfer* **110** 62–71
- [49] Farley D R 2010 *J. Chem. Phys.* **133** 094303
- [50] Briefi S, Mattei S, Lettry J and Fantz U 2017 *AIP Conf. Proc.* **1869** 030016